

# A Compact Circularly Polarized Rotated L-Shaped Antenna with J-Shaped Defected Ground Structure for WLAN and V2X Applications

Jayshri Kulkarni<sup>1, \*</sup>, Chow-Yen-Desmond Sim<sup>2</sup>, Ajay Poddar<sup>3</sup>,  
Ulrich L. Rohde<sup>3</sup>, and Abdullah G. Alharbi<sup>4</sup>

**Abstract**—A novel and compact microstrip-line fed printed antenna for wideband circular polarization (CP) radiation is proposed. The designed antenna utilizes a crescent-shaped substrate, rotated L-shaped monopole, and defected ground structure (DGS) to achieve a wide 3-dB axial ratio (AR) bandwidth and 10-dB impedance bandwidth (ZBW) across the entire 5 GHz Wireless Local Area Network (WLAN) and Vehicle to Everything (V2X) operational bands. As the substrate of the proposed antenna is only 0.8 mm thick, it has a very low profile of  $0.014\lambda$  in terms of free space wavelength ( $\lambda$ ) at 5.5 GHz. The proposed CP antenna exhibits overlapping 10-dB ZBW and 3-dB AR bandwidth (ARBW) of 22.05% (4.80–5.99 GHz), along with broadside far-field patterns, gain greater than 2.5 dBi, and efficiency above 85% throughout the desired operating band. Therefore, it is a good candidate for WLAN and V2X communication applications.

## 1. INTRODUCTION

The CP radiation and high radiating performance antennas with their favorable features such as low profile, light weight, and planner structure are very essential for modern wireless communication including Industrial Internet of Things (IIoT), machine to machine communication in aerospace, security, commercial, agricultural as well as V2X applications [1, 2]. In this context, several antenna designers and researchers have reported outstanding CP/dual CP antennas to meet the growing demand for broad bandwidth and multimedia applications in the near future [3–18]. Among them, slots with various geometries of the radiating element are gaining more attention [3–18] as they can be utilized to generate CP radiations easily for desired wireless bands.

The antenna reported in [3] is designed using an asymmetrical Y-shaped DR material for WLAN and WiMAX operations with a designed footprint of  $120 \times 70 \text{ mm}^2$ , whereas a CP dual-band modified  $\Psi$ -shaped antenna that has a dimension of  $130 \times 85 \text{ mm}^2$  is discussed in [4]. However, both antennas have very large dimensions. Antennas with reduced footprint are discussed in [5–7]. The annular ring slot antenna in [5] is designed on a  $50.3 \times 51.5 \text{ mm}^2$  Teflon substrate whereas the perturbed psi-shaped antenna in [6] and fractal inspired slot antenna in [7] are printed on  $58.2 \times 47.7 \text{ mm}^2$  RT-Duroid and  $39 \times 46 \text{ mm}^2$  TLY-5 substrate, respectively. Even though the CP antennas in [5–7] have exhibited small dimensions and dual-band operations, they are designed on expensive substrates.

To reduce the cost, the antennas in [8–11] are designed on cost-effective and easily available FR-4 substrate. Here, a fan-shaped CP antenna operating in the 2.4 GHz WLAN band is reported in [8], while [9] has reported a fractal defected ground patch antenna operating in the 1.55 GHz band. In [10], a

---

*Received 3 January 2022, Accepted 28 January 2022, Scheduled 4 February 2022*

\* Corresponding author: Jayshri Kulkarni (jayah2113@gmail.com).

<sup>1</sup> Department of Electronics and Telecommunication Engineering, Vishwakarma Institute of Information Technology, Pune, India.

<sup>2</sup> Department of Electrical Engineering, Feng Chia University, Taiwan. <sup>3</sup> Synergy Microwave Corp, Paterson, NJ, USA. <sup>4</sup> Jouf University, Sakaka, Saudi Arabia.

truncated square aperture patch antenna operating in the 2.4/5 GHz WLAN band has been investigated, whereas a gap coupled patch antenna operating in the 3.6/5.3 WLAN/WiMAX band is discussed in [11]. However, the antennas in [8–11] have demonstrated a very narrow ZBW and do not cover the entire band of operation. Wideband antennas designed on cost-effective FR-4 substrate have been reported in [12–16]. The square slot CP antenna in [12] has a ZBW of 36.41% (4.65–6.72 GHz), and the perturbation patch antenna with open slot [13] has shown a very wide ZBW of 103.5% (2.40–7.55 GHz). Notably, the inverted L-shaped CP antenna design in [14] has demonstrated a wide ZBW of 50.9% (3.48–5.86 GHz) for C-band application, and the CP microstrip dual-band antenna (with L-shaped radiator and two circular strips) studied in [15] has also shown wide ZBWs of 46.4% (1.82–2.92) and 40.5% (3.15–4.75 GHz). Nonetheless, to cover both Sub-6 GHz and X-band applications, [16] has reported a uniplanar slot antenna with a loaded metallic reflector at the bottom, and dual broadband ZBWs of 21.27% (5.46–6.76 GHz) and 24.65% (8.18–10.48 GHz) were achieved. Even though the antennas in [12–16] have also achieved wide ZBWs, they do not have matching overlapping ARBW. A frequency tunable dual folded inverted-L CP antenna [17] and CP V-shaped slot antenna [18] with overlapping 3-dB ARBW and 10-dB ZBW have been investigated recently; however, the use of diodes and vias in [17] and [18], respectively, have increased their manufacturing complexity.

Compared with the aforementioned various CP antenna techniques, the proposed CP antenna design is a simple patch design that is composed of a microstrip-line fed rotated L-shaped antenna with J-shaped DGS, and it has a very wide overlapping 3-dB ARBW and 10-dB ZBW. In this design, a non-centered rotated L-shaped strip and J-shaped DGS (narrow slit and slots) are etched on the upper and bottom layers of the crescent-shaped FR-4 substrates, respectively, to generate very wide impedance matching and CP characteristics across the entire 5 GHz WLAN and V2X band. By utilizing the above structure, near overlapping 3-dB ARBW and 10-dB ZBW of 31.5% (4.80–5.99 GHz) are achieved. As the proposed CP antenna has exhibited the antenna gain of greater than 2.5 dBi, efficiency above 85%, and desirable CP radiations across the entire 5 GHz WLAN and V2X band, it is a very suitable CP antenna design for modern wireless communications.

## 2. GEOMETRY AND DESIGN OF PROPOSED ROTATED L-SHAPED ANTENNA

Figures 1(a) and 1(b) show the geometry of the proposed CP antenna that is printed on a lossy 0.8 mm thick crescent-shaped FR-4 dielectric with dielectric constant ( $\epsilon_r$ ) of 4.3 and loss tangent ( $\tan \delta$ ) of 0.025. Its corresponding layered view is depicted in Figure 1(c). The optimized dimensions of the proposed CP antenna are articulated in Table 1, and it has a volume size of  $30 \times 30 \times 0.8 \text{ mm}^3$  ( $0.55 \times 0.55 \times 0.014\lambda^3$ ). The upper surface layer of the crescent-shaped FR-4 substrate is composed of a non-centered rotated L-shaped monopole excited by a  $50 \Omega$  microstrip transmission feeding line, while the bottom surface layer is mainly a J-shaped DGS, as shown in Figures 1(a) and 1(b), respectively. Here, the  $50 \Omega$  microstrip feeding line has a size of  $(L_F \times W_F)$ , and it is deployed at a distance of  $W_a$ , located on the left edge

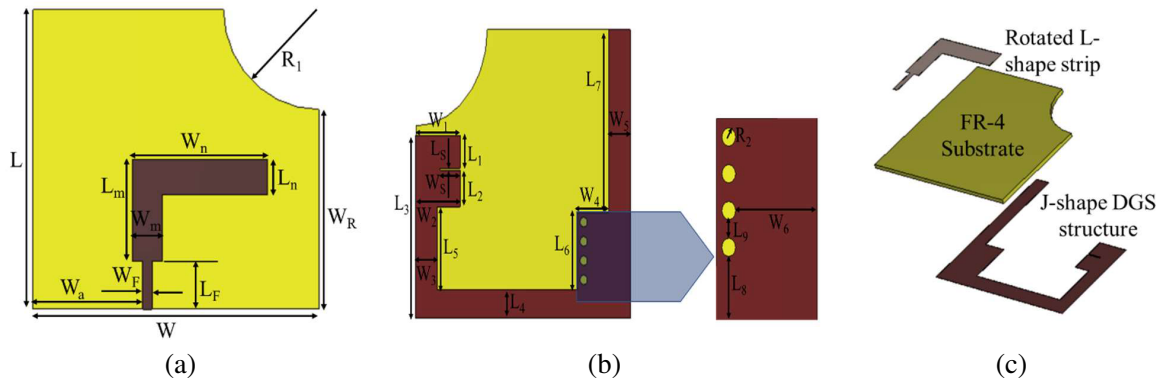


**Figure 1.** Geometry of the proposed CP antenna (all dimensions are in mm), (a) front View, (b) back View, (c) layered View.

**Table 1.** Optimized dimensions of the proposed CP antenna.

Parameters	Values (mm)	Parameters	Values (mm)	Parameters	Values (mm)
$L$	30.0	$L_7$	19.0	$W_1$	6.2
$L_F$	4.8	$L_8$	3.5	$W_2$	6.2
$L_m$	10.2	$L_9$	1.0	$W_3$	3.0
$L_n$	3.5	$L_S$	0.2	$W_4$	4.4
$L_1$	3.4	$W$	30.0	$W_5$	3.0
$L_2$	3.8	$W_F$	1.0	$W_6$	6.0
$L_3$	19.0	$W_m$	3.2	$W_S$	2.8
$L_4$	3.0	$W_n$	14.2	$R_1$	10
$L_5$	8.6	$W_a$	11	$R_2$	0.5
$L_6$	8.0	$W_R$	20.0		

of the substrate. As for the rotated L-shaped monopole that is connected to the microstrip feeding line, it has vertical and horizontal sections of size  $(L_m \times W_m)$  and  $(L_n \times W_n)$ , respectively, as seen in Figure 1(a). As depicted in Figure 1(b), the left opening stub section of the J-shaped DGS is composed of two rectangular stubs of sizes  $(L_1 \times W_1)$  and  $(L_2 \times W_2)$ , and a very narrow slit of size  $(L_s \times W_s)$  is loaded into this opening stub section. Here, a vertical rectangular stub of size  $(L_5 \times W_3)$  is linked to the bottom of this left opening stub section, and it is connected to a horizontal bottom stub of size  $(W \times L_4)$ . Notably, the right section of the J-shaped DGS is composed of two vertical stubs, in which the narrow opening vertical stub has a size of  $(L_7 \times W_5)$ , and the bottom right-side stub section can be considered as a protruded rectangular stub section of size  $(L_6 \times W_4)$ , in which four identical circular slots (with radius  $R_2$  spaced at a distance  $L_9$  from each other) are vertically loaded into this protruded rectangular section, so as to achieve good impedance matching and CP radiations across the 5 GHz WLAN and V2X bands. As for the crescent cut (with radius  $R_1$ ) at the top-right corner of the FR-4 substrate, it is to further achieve wide ZBW and ARBW across the desired operating bands. The proposed CP antenna is simulated and optimized using CST MWS software<sup>®</sup> [19].

### 3. STEP-WISE EVOLUTION OF THE PROPOSED CP ANTENNA

The step-wise design evolution to analyze the working mechanism of the proposed CP antenna is depicted in Figure 2 and Figure 3, showing the reflection coefficient ( $S_{11}$ ) and 3-dB AR curves, respectively. Initially, as shown in Figure 2, in Step-1, a vertical non-centered rectangular strip along with a rotated L-shaped monopole fed by a microstrip line with partial J-shaped DGS is designed. In Step-2, a narrow slit ( $L_s \times W_s$ ) is further loaded into the left opening section of the J-shaped structure. In Step-3, the

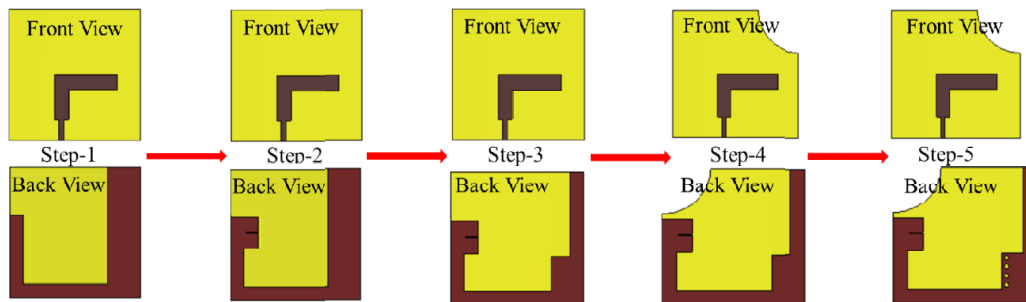


**Figure 2.** Step-wise design evaluation of the proposed CP antenna.

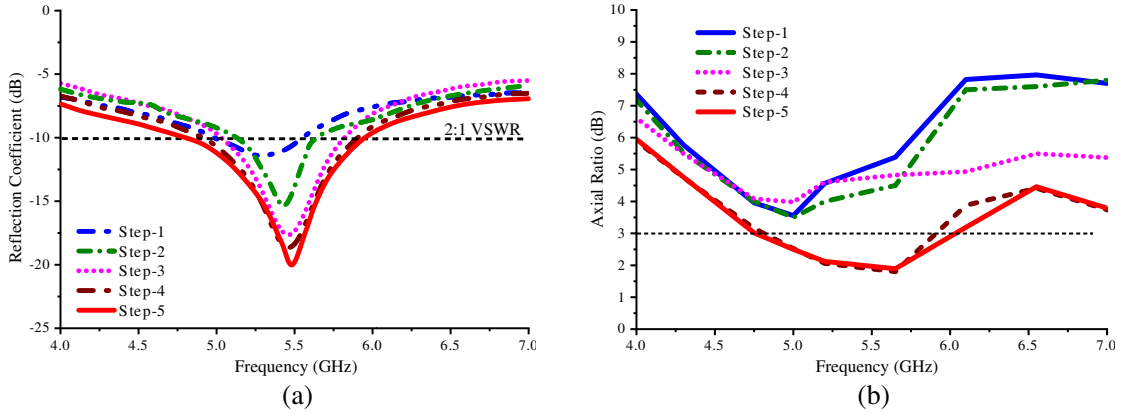


**Figure 3.** Step-wise design of the proposed CP antenna, (a)  $S_{11}$  (dB), (b) Axial Ratio.

right vertical section is reduced to two non-equal width vertical stubs, and it can be regarded that the bottom right corner has a protruded rectangular stub section ( $L_6 \times W_4$ ). Next, in Step-4, the top right corner of the FR-4 substrate is removed with a size of a quarter-circle that has a radius of  $R_1$ . Finally, in Step-5, four vertical circular slots (each with radius  $R_2$ ) are loaded into the protruded rectangular stub section.

The  $S_{11}$  and AR curves based on the step-wise evolution from Step-1 to Step-5 of the proposed CP antenna are analyzed in Figures 3(a) and 3(b), respectively. It is apparent that the antenna in Step-1 induces a linear polarization (LP), and it has a very narrow bandwidth. In Step-2 and Step-3, the deployment of the two rectangular stubs (separated by the narrow slit) and the protruded rectangular stub section placed at the bottom right corner of the J-shaped structure which perturbs the current paths have aided in generating more electric field current that results in enhancing the 10-dB ZBW. Here, even though a significant increase in the bandwidth is noticed, the antenna is linearly polarized, and the desired 5 GHz WLAN band is not covered. It is further noticed from Figure 3(b) that desirable CP bandwidth performances (with AR < 3 dB) are achieved by removing the top-right corner of the substrate with a quarter-circle of radius  $R_1$ . Finally, the four vertical circular slots can aid in achieving the desired 10-dB ZBW and 3-dB ARBW of 22.55% (4.76–5.97 GHz).

#### 4. SURFACE CURRENT DISTRIBUTION FOR UNDERSTANDING THE CP MECHANISM

To fathom how the CP radiation is excited, it can be easily observed (at the resonating frequency of 5.5 GHz) by determining the rotation of the resultant surface current distribution ( $J$ ) A/m at phase angle  $0^\circ$  and  $90^\circ$ , as shown in Figures 4(a) and 4(b), respectively. The surface current is observed on the rotated L-shaped monopole on the front side as well as on the J-shaped strip on the backside. Here, it is apparent that the resultant current  $J$  lies in the second and third quadrants at phase angles of  $0^\circ$  and  $90^\circ$ , respectively. It can be noticed that the resultant current  $J$  rotates in a counterclockwise direction and orthogonal to each other as the phase changes from  $0^\circ$  to  $90^\circ$ . Therefore, as the resultant current rotates in a counterclockwise direction, a right-hand CP (RHCP) is achieved.

#### 5. RESULTS AND DISCUSSION OF THE PROPOSED CP ANTENNA

The proposed CP antenna was fabricated, and its corresponding top and bottom views are shown in Figures 5(a) and 5(b), respectively. The prototype was validated by measuring the scattering and radiation performances. Here, the scattering performance was validated by using the ROHDE & SCHWARZ (9 kHz–16 GHz) Network Analyzer, while the radiation performances (including radiation patterns, gain, and radiation efficiency) were achieved in a calibrated anechoic chamber, as shown in Figure 5(c).

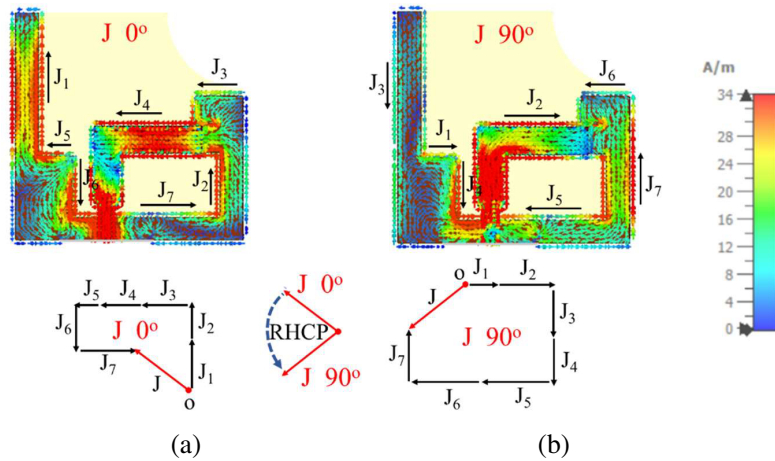


**Figure 4.** Simulated Surface current (A/m) distribution of the proposed CP antenna at 5.5 GHz (a) at 0°, (b) at 90°.

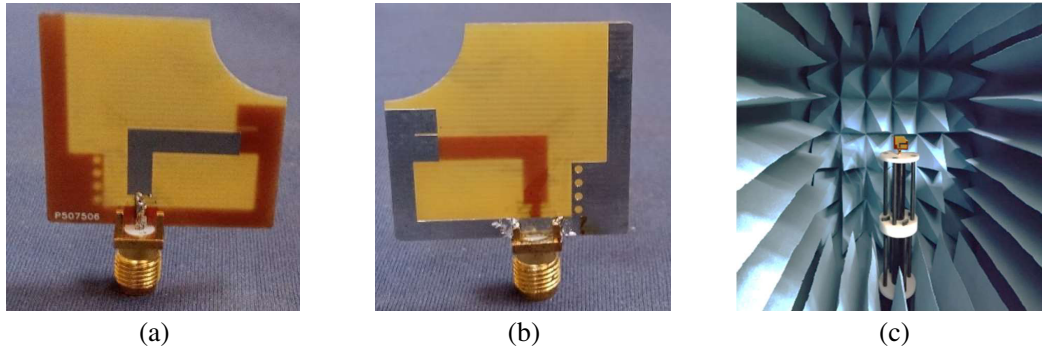


**Figure 5.** Fabricated prototype and measurement set-up of the proposed CP antenna, (a) front view, (b) back view, (c) antenna mounted inside anechoic chamber.

**5.1. Reflection Coefficient ( $S_{11}$ ) dB and 3-dB Axial Ratio Bandwidth (ARBW)**

Figure 6(a) shows the simulated and measured  $S_{11}$  of the proposed CP antenna. The simulated and measured 10-dB ZBW are 22.55% (4.76–5.97 GHz) and 22.05% (4.80–5.99 GHz). Compared with Figure 6(b), it is noticed that a wide CP bandwidth is achieved across the desired band of interest. The simulated and measured 3-dB ARBWs of the proposed CP antenna are 22.55% (4.76–5.97 GHz) and 22.05% (4.80–5.99 GHz). It can be observed that the 10-dB ZBW and 3-dB ARBW completely overlap with each other. Notably, a very slight deviation between the simulated and measured results is noticed, which may be due to a slight fabrication tolerance of the proposed CP antenna prototype.

**5.2. Radiation Patterns of the Proposed CP Antenna**

Figure 7 shows the comparison of two-dimensional (2D) simulated and measured radiation patterns of the proposed CP antenna (at 5.5 GHz) in the  $xz$ -plane ( $E$ -plane) and  $yz$ -plane ( $H$ -plane). Here, one can see that the left-hand circularly polarized (LHCP) waves excited by the proposed CP antenna are tilted at a  $\pm 30^\circ$  broadside direction, whereas the right-hand circularly polarized (RHCP) waves are excited at  $\pm 120^\circ$  of LHCP. A slight deviation in the measured and simulated results is observed, which may be due to fabrication tolerances and the use of coaxial cable inside the anechoic chamber.

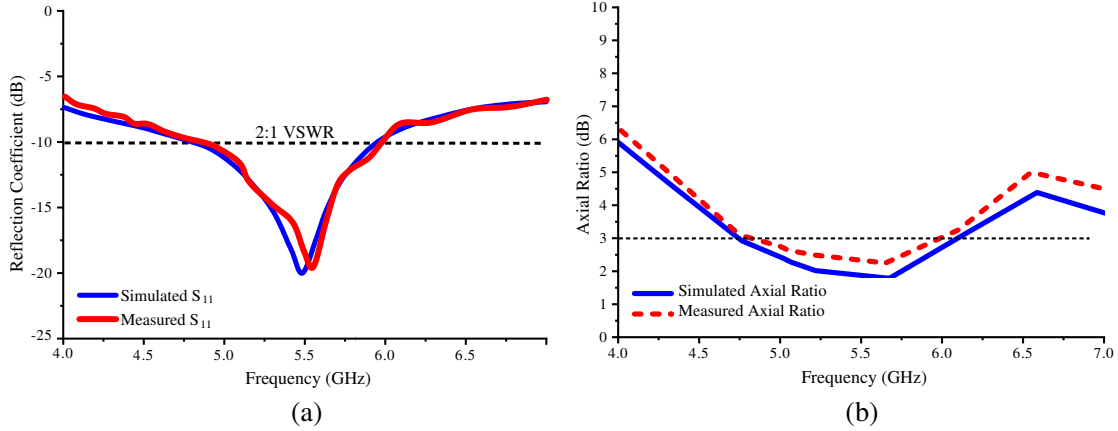


**Figure 6.** Measured and simulated results of the proposed CP antenna, (a)  $S_{11}$  (dB), (b) Axial Ratio (dB).

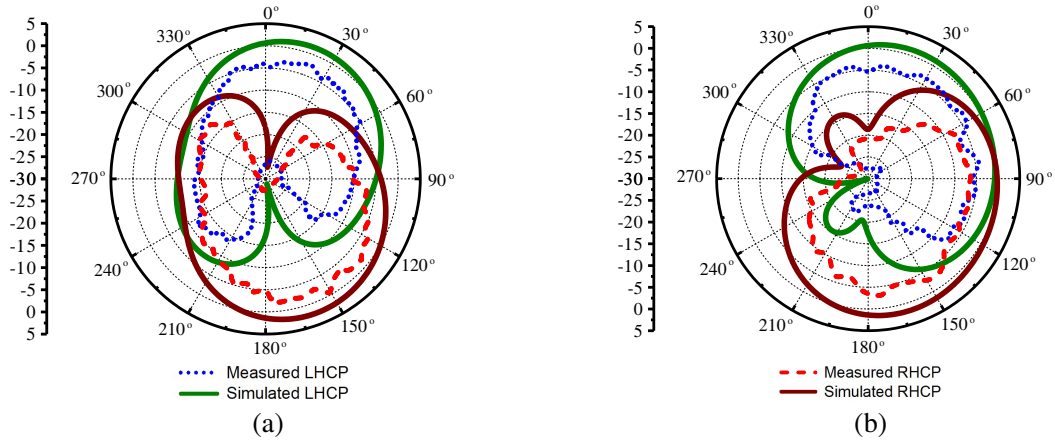


**Figure 7.** Measured and Simulated 2D radiation pattern of the proposed CP antenna at 5.5 GHz, (a)  $E$ -plane, (b)  $H$ -plane.

### 5.3. Measured and Simulated Gain and Radiation Efficiency

Figure 8 shows the gain and efficiency curves of the proposed CP antenna. The simulated gain was calculated using Friss Formula given in [20]. As shown in Figure 8, measured gain ranging between 2.5 dBi and 3.5 dBi is observed, whereas the simulated gain is  $> 3$  dBi throughout the operating band. Likewise, the measured and simulated efficiencies were above 85% and 88%, respectively, across the band of interest.

## 6. PERFORMANCE COMPARISON OF THE PROPOSED CP ANTENNA

Table 2 shows the performance comparison of the proposed CP antenna with other existing reported state of the arts, which include size, 10-dB ZBW, 3-dB ARBW, gain, and antenna design technique.

As depicted in Table 2, the salient features of the proposed CP antenna are listed as follows:

1. Compared to all the reported state of the art, the proposed CP antenna is compact in size (occupies the smallest area), unlike [1–11] and [13–18].
2. Unlike [3, 4, 16], it does not require any additional ground plane, reactive component, or a 3-dimensional structure for the excitation of bands.
3. It does not use expensive substrate as compared to [3, 5–7].

**Table 2.** Performance comparison of the proposed CP antenna.

Ref	Size (mm <sup>2</sup> )	Thickness (mm)	ZBW (GHz)	ARBW (GHz)	Substrate	Gain	Antenna Design
1	63 × 58.4	1.5	1.5–3.3	1.98–3.02	FR-4	2.5	Chifre shaped monopole along with asymmetric fed
2	60 × 50	0.8	2.21–2.86 5.05–6.54	2.24–2.56 5.01–5.94	FR-4	2.33	annular-slot antenna loaded with a lightning-shaped slot
3	120 × 70	20.5	2.20–4.18	2.38–2.5	Taconic RF-35	4.11	Y-shaped DR Antenna
4	130 × 85	6.6	3.4–4.8	3.48–3.92 4.54–4.77	FR-4	7	Modified Ψ Shape
5	50.3 × 51.5	0.5	5.4–7.0	5.67–5.97	Teflon	7.6	Annular Ring with u-shaped Slot Antenna
6	58.2 × 47.7	0.254	5.0–7.0	4.9–5.7	RT-Duroid	7	Perturbed PSI-shaped Antenna
7	39 × 46	1.6	3.43–4.64 5.08–9.00	3.26–3.91 6.33–8.49	TLY-5	2	CPW-Fed Fractal Inspired wide slot antenna
8	38 × 42	1.6	2.4–2.484	2.43–2.46	FR-4	-	Circular disc sector patch is truncated to obtain fan shape
9	45 × 45	3.18	1.55–1.58	1.572–1.578	FR-4	1.7	Etched Fractal Defected Ground
10	40 × 54	1.6	2.40–2.48 5.72–5.87	2.40–2.49 5.58–5.93	FR-4	3	Truncated square aperture slot
12	21.8 × 20	0.74	4.65–6.72	4.85–5.37	FR-4	3	Square slot with modified corner at the left-bottom of the square slot and two orthogonal equal size patches
14	32 × 32	1.6	3.48–5.86	4.71–5.54	FR-4	5	Inverted L-shape Antenna with slits, notch, square, strips and stubs on the ground plane
15	45 × 45	1.0	1.82–2.92 3.15–4.75	1.88–2.42 3.20–4.83	FR-4	4.8	Upper L-Shaped radiator and two circular strips on the ground
16	60 × 60	9.66	5.46–6.76 8.18–10.48	5.7–6.25 8.55–10	FR-4	7	Metallic Reflector & RF pin diode
17	66 × 10	1	3.28–3.70 6.42–6.75 13.75–14.2	3.28–3.70 6.42–6.75 13.75–14.2	FR-4	2.68	Frequency Tunable Dual Folded Inverted L antenna with varactor loaded split ring resonator structures
18	42 × 44	0.8	2.19–4.6	2.19–4.6	FR-4	-	Z-shaped feedline and two right angled V-slot
Proposed	30 × 30	0.8	4.80–5.99	4.80–5.99	FR-4	2.5	Rotated L-shaped monopole and J-shaped defected ground structure (DGS)

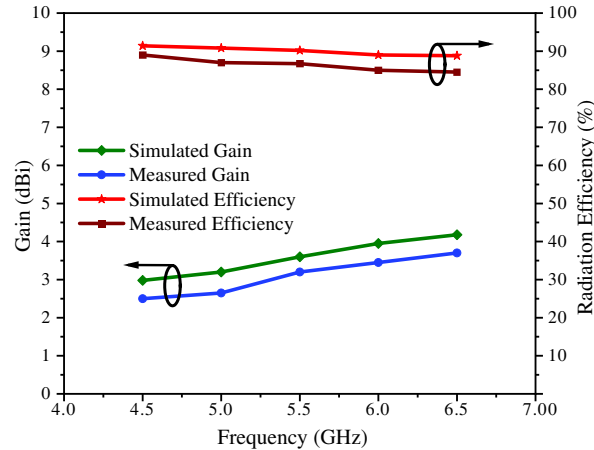


**Figure 8.** Gain and efficiency plots of the proposed CP antenna.

4. The proposed CP antenna is very compact and has very wide ZBW and ARBW, unlike [8–10].
5. The 3-dB ARBW overlaps with the 10-dB ZBW, meaning that the operating CP bandwidth is very wide and comparable with the excited ZBW, which is a unique feature. In comparison, the 3-dB ARBW in [1–16] is much narrower than the 10-dB ZBW.

## 7. CONCLUSION

A novel CP antenna for 5 GHz WLAN and V2X communication with CP radiation has been studied successfully. The proposed CP antenna has a simple geometry and a very small designed footprint of  $30 \times 30 \text{ mm}^2$ . It is also easy to fabricate, less costly, and can be easily integrated into any wireless device with restricted space. The proposed CP antenna exhibits a measured 3-dB ARBW of (4.8–5.99 GHz) with overlapping measured 10-dB ZBW. The antenna also exhibits broadside radiation patterns, gain above 2 dBi, and efficiency greater than 85% throughout the operating band. This confirms the applicability of the proposed CP antenna design for 5 GHz WLAN and V2X communication.

## REFERENCES

1. Han, R. C. and S. S. Zhong, “Broadband circularly-polarised chifre-shaped monopole antenna with asymmetric feed,” *Electron. Lett.*, Vol. 52, No. 4, 256–258, Feb. 2016.
2. Ge, L., C. Y. D. Sim, H. L. Su, J. Y. Lu, and C. Ku, “Single-layer dual-broadband circularly polarised annular-slot antenna for WLAN applications,” *IET Microw. Antennas Propag.*, Vol. 12 No. 1, 99–107, 2018.
3. Altaf, A. and M. Seo, “Dual-band circularly polarized dielectric resonator antenna for WLAN and WiMAX applications,” *Sensors*, Vol. 20, No. 4, 1137, Feb. 2020.
4. Deshmukh, A. A. and A. A. Odhekar, “Dual band circularly polarized modified  $\Psi$ -shape microstrip antenna,” *Progress In Electromagnetics Research C*, Vol. 115, 161–174, 2021.
5. Rasool, N., H. Kama, M. Abdul Basit, and M. Abdullah, “A low profile high gain ultra lightweight circularly polarized annular ring slot antenna for airborne and airship applications,” *IEEE Access*, Vol. 7, 155048–155056, 2019.
6. Mondal, T., S. Maity, R. Ghatak, and S. R. B. Chaudhuri, “Design and analysis of a wideband circularly polarised perturbed psi-shaped antenna,” *IET Microw. Antennas Propag.*, Vol. 12, No. 9, 1582–1586, 2018.
7. Saraswat, K. and A. R. Harish, “A dual band circularly polarized  $45^\circ$  rotated rectangular slot antenna with parasitic patch,” *International Journal of Electronics and Communications*, Vol. 123, 2020, doi: <https://doi.org/10.1016/j.aeue.2020.153260>.

8. Mathew, S., R. Anitha, P. V. Vinesh, and K. Vasudevan, "Circularly polarized sector-shaped patch antenna for WLAN applications," *Procedia Computer Science*, Vol. 46, 1274–1277, 2015.
9. Wei, K., J. Y. Li, L. Wang, R. Xu, and Z. J. Xing, "A new technique to design circularly polarized microstrip antenna by fractal defected ground structure," *IEEE Transactions on Antennas and Propagation*, Vol. 65, No. 7, 3721–3725, Jul. 2017.
10. Niyamanon, S., R. Senathong, and C. Phongcharoenpanich, "Dual-frequency circularly polarized truncated square aperture patch antenna with slant strip and L-shaped slot for WLAN applications," *International Journal of Antennas and Propagation*, Vol. 2018, 1–11, 2018.
11. Singh, V., B. Mishra, and R. Singh, "Anchor shape gap coupled patch antenna for WiMAX and WLAN applications," *COMPEL — Int. J. Comput. Math.*, Vol. 38, 263–286, 2019.
12. Midya, M., S. Bhattacharjee, and M. Mitra, "Compact CPW-fed circularly polarized antenna for WLAN application," *Progress In Electromagnetics Research M*, Vol. 67, 65–73, 2018.
13. Fu, Q., Q. Feng, and H. Chen, "Design and optimization of CPW-fed broadband circularly polarized antenna for multiple communication systems," *Progress In Electromagnetics Research Letters*, Vol. 99, 65–74, 2021.
14. Srivastava, K., B. Mishra, and R. Singh, "Microstrip-line-fed inverted L-shaped circularly polarized antenna for C-band applications," *International Journal of Microwave and Wireless Technologies*, 1–9, 2021, doi: <https://doi.org/10.1017/S1759078721000635>.
15. Yu, Z., L. Huang, Q. Gao, and B. He, "A compact dual-band wideband circularly polarized microstrip antenna for sub-6G application" *Progress In Electromagnetics Research Letters*, Vol. 100, 99–107, 2021.
16. Mohanty, A. and B. R. Behera, "Dynamically switched dual-band dual-polarized dual-sense low-profile compact slot circularly polarized antenna assisted with high gain reflector for sub-6 GHz and X-band applications," *Progress In Electromagnetics Research C*, Vol. 110, 197–212, 2021.
17. Praveen Kumar, P. C. and P. T. Rao, "Frequency-tunable circularly polarized twin dual folded inverted-L antenna with varactor-loaded split-ring resonator structures," *Int. J. Commun. Syst.*, e4715, 2021, <https://doi.org/10.1002/dac.4715>.
18. Huang, H. F. and B. Wang, "A circularly polarized slot antenna with enhanced axial ratio bandwidth," *2017 Sixth Asia-Pacific Conference on Antennas and Propagation (APCAP)*, 1–3, 2017.
19. CST-Computer Simulation Technology Studio Suite, 2017, <https://www.cst.com2017>.
20. Kulkarni, J., "Multi-band printed monopole antenna conforming bandwidth requirement of GSM/WLAN/WiMAX standards," *Progress In Electromagnetics Research Letters*, Vol. 91, 59–66, 2020.